Cortical Thickness Measurement from Magnetic Resonance Images Using Partial Volume Estimation

Maria A. Zuluaga[a,b], Oscar Acosta[a], Pierrick Bourgeat[a], Marcela Hernández Hoyos[b], Olivier Salvado[a], and Sébastien Ourselin[a,c]

[a] BioMedIA Lab, eHRC, ICT Centre, CSIRO, Level 20 300 Adelaide Street, Brisbane, Australia;
[b] Grupo IMAGINE, Grupo Ingeniería Biomédica, Universidad de los Andes, Cra 1 No. 18A 10, Bogotá, Colombia
[c] Department of Computer Science, University College London, London, United Kingdom

ABSTRACT

Measurement of the cortical thickness from 3D Magnetic Resonance Imaging (MRI) can aid diagnosis and longitudinal studies of a wide range of neurodegenerative diseases. We estimate the cortical thickness using a Laplacian approach whereby equipotentials analogous to layers of tissue are computed. The thickness is then obtained using an Eulerian approach where partial differential equations (PDE) are solved, avoiding the explicit tracing of trajectories along the streamlines gradient. This method has the advantage of being relatively fast and insure unique correspondence points between the inner and outer boundaries of the cortex. The original method is challenged when the thickness of the cortex is of the same order of magnitude as the image resolution since partial volume (PV) effect is not taken into account at the gray matter (GM) boundaries. We propose a novel way to take into account PV which improves substantially accuracy and robustness. We model PV by computing a mixture of pure Gaussian probability distributions and use this estimate to initialize the cortical thickness estimation. On synthetic phantoms experiments, the errors were divided by three while reproducibility was improved when the same patients was scanned three consecutive times.

Keywords: segmentation, thickness estimation, partial volume effect

1. INTRODUCTION

The cerebral cortex is a sheet of gray matter (GM) located on the outer surface of the brain. Measurement of the cortical thickness from 3D magnetic resonance (MR) images can aid diagnosis and longitudinal studies of a wide variety of neurodegenerative and psychiatric disorders, such as Alzheimer's disease, schizophrenia and epilepsy.

The accuracy of the thickness estimation is limited by the partial volume effect (PVE), where the resolution of MR image is such that voxels may consist of more than one tissue type. Due to PVE, the classification of a voxel reflecting the dominant tissue type, does not reveal all possible tissue content of that voxel and PVE results in a loss of accuracy. We define the gray matter/white matter (WM) interface as the inner boundary of the cortex, and the gray matter/cerebrospinal fluid (CSF) interface as the outer boundary. Niessen *et al.*[1] showed that consistently misplacing by a single pixel the tissue borders in a 1 mm^3 isotropic MR brain image in each slice resulted in volume errors of approximately 30%, 40% and 60% for WM, GM, and CSF respectively. Ballesteros *et al.*[2] showed also that PVE and discrete sampling at boundary locations lead to volume measurement errors in the range of 20%-60%. We are thus working on estimating of the fractional content of each tissue type to correct the estimation of boundary location, with the goal of improving the accuracy of the cortical thickness measurement.

PV estimation has been tackled for MR segmentation following two different approaches. First, several studies[3–5] assumed that all the voxels in the image were subject to PVE and that the fractional content proportions changed smoothly across the image. The smoothing constraint was imposed by a Markov Random Field model. The second approach, originally proposed by Santago and Gage,[6] did not take into account the spatial dependence of the tissue fractions between the voxels, but explicitly assumed a uniform prior probability for all mixed tissues. Their approach derived the intensity distribution for PV between two normally distributed tissue types.

Medical Imaging 2008: Image Processing, edited by Joseph M. Reinhardt, Josien P. W. Pluim,
Proc. of SPIE Vol. 6914, 69140J, (2008)
1605-7422/08/$18 · doi: 10.1117/12.770058

Santago and Gage only addressed the problem of estimating the total volume of each tissue for a entire brain. Other authors[7–10] have extended the method to estimate the amount of every tissue in each individual voxel. This extension, referred as indirect,[10] assumed that each voxel contained at most two types of tissue when only one MRI contrast was available. The methods identified the two tissue types present in each voxel followed by the estimation of their fractional content. All of the mentioned methods have been proposed for improving tissue segmentation, but to our knowledge none were incorporated into a framework to improve cortical thickness estimation.

Indeed, our objective is to increase the accuracy and robustness of the cerebral cortical thickness measurement using PV estimated from MRI T1W. We improved upon the Laplacian method to measure cortical thickness originally published by Jones *et al.*[11] with the Eulerian implementation of Yezzi and Prince.[12] Because the GM thickness is only about three millimeters and the MRI resolution is $1mm^3$ isotropic, significant PV is present at the GM boundaries with CSF and WM. The original method used binary segmented masks which introduced up to 6% error on our test with a hollow spherical synthetic phantom. This error is too important for measuring atrophy between mild cognitive impairment and Alzheimer's disease patients reported to be between 10-20% in[13] for example. This paper presents a novel extension of Jones' *et al.*[11] method to estimate cortical thickness which takes into account PV using fractional tissue content estimated from a tissue classification step.

In section 2 we describe the proposed model for thickness estimation correction with the inclusion of PV. Section 3 presents the validation method and experimental results. Finally, in Section 4 we discuss important points of our method and conclude.

2. METHOD

In the first step, we segmented the three pure tissue classes (GM, WM, CSF) plus the background using a maximum likelihood (ML) algorithm.[14] Next, we modeled two mixed classes (GM/WM and GM/CSF) and the image was segmented using a Markov random field technique. Once the PV voxels were segmented, we computed their mixture of pure tissues. In a second step we initialized the cortical thickness estimation with the tissue mixture and integrated following the gradient of the Laplacian equation using partial differential equations.

2.1 Pure Tissue Segmentation Using The Expectation-Maximization Algorithm

The input MR T1W image was segmented using the expectation maximization segmentation algorithm proposed by Van Leemput *et al.*[14] The intensity histogram of the MR image was modeled as a mixture of Gaussian distributions. The expectation-maximization (EM) algorithm was used to iteratively update the model parameters and tissue classifications in order to maximize the likelihood of the image data. Bias field correction and a Markov random field to increase robustness to noise noise were included in the EM algorithm. We then performed a maximum *a posteriori* (MAP) classification by assigning each voxel to its most likely tissue type. Hard segmentations (Figure 1(a)) and resulting mean μ_j and covariance matrix Σ_j, of every tissue class j were used as an input for the following partial volume estimation stage.

2.2 Partial Volume Estimation

For estimating the partial volume of each voxel, three pure classes (GM, WM and CSF) were considered and two mixture classes: GM/CSF and GM/WM. The Background was excluded from the analysis as it was assumed to be correctly segmented by the EM algorithm. We assumed also that the EM algorithm segmented correctly pure voxels. Since voxels containing partial volume were mostly present along inner and outer boundaries, PV evaluation was performed on a region formed by the dilated gray matter masks generated from the previous MAP classification.

Two different tissue models were considered, one for pure tissues and one for voxels containing a mixture of two tissue types. Pure tissue intensities were modeled using a single Gaussian probability density function. Voxels containing a mixture of two tissue types were modeled with a probability density function proposed by Santago and Gage[6] and computed numerically from normal distribution parameters of the pure tissues:

$$p(x_i|c_i = \{j,k\}) = \int_0^1 \frac{1}{\sqrt{2\pi det(\Sigma(w))}} exp\left[-\frac{1}{2}(x_i - \mu(w))^T \Sigma^{-1}(x_i - \mu(w))\right] \quad (1)$$

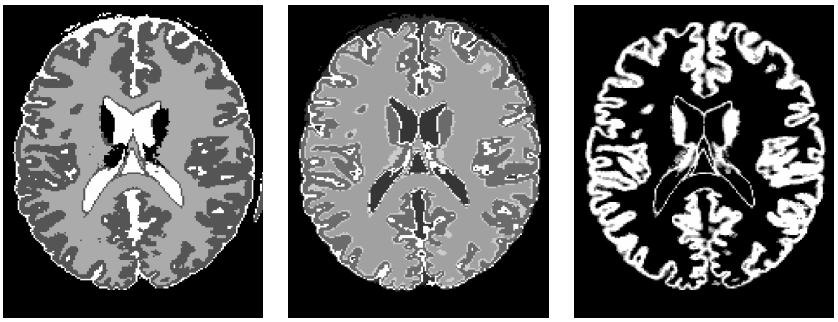

(a) (b) (c)

Figure 1. (a) Initial hard segmentation. (b) Refined hard segmentation including PV classes. (c) Grey matter PV map.

where

$$\mu(w) = w\mu_j + (1-w)\mu_k; \Sigma(w) = w^2\Sigma_j + (1-w)^2\Sigma_k, \tag{2}$$

c_i denotes the class of a mixed voxel x_i formed by classes j and k, and w represents the fractional content.

Given the observed intensity of a voxel x_i, the probability of this voxel belonging to any of the five classes was computed using a mixture of the Gaussian distributions for the pure tissues and the computed probability density functions of the two PV tissue models. A new MAP classification was computed. To take into account spatial correlation between voxels, we included a Markov random field model using a labeling performed using a Potts model:[8]

$$p(\Lambda) = \frac{1}{Z} exp\left(-\beta \sum_i \sum_{k \in N_i} \delta(\lambda_i, \lambda_k)\right), \tag{3}$$

where Λ is the labeled image, N_i represents the voxels in the neighborhood of voxel i, Z is a scaling constant, λ_i and λ_k are the labels (classification) of the voxels i and k and β controls the strength of the prior. Using a Bayesian formulation, we aimed to find the labeled image Λ with the highest conditional probability. We use the ICM algorithm[15] to search for the optimal labeling.

Once voxels were classified as PV (Figure 1(b)), their fractional content (Figure 1(c)) was computed using the bias corrected intensity $\bar{x}_i$, and the means of the corresponding two pure tissue types μ_j and μ_k:

$$f_k = U\left(\frac{\mu_j - \bar{x}_i}{\mu_j - \mu_k}\right) \tag{4}$$

where $U(\cdot)$ is a limiter restricting the range of the fractional content to $[0, 1]$.

We used the resulting means and covariance matrices of the EM algorithm (Section 2.1) to initialize the PV estimation and estimate the labelling.

2.3 Thickness estimation without PV model

In the original method by Jones *et al.*,[11] binary masks for GM, WM, and CSF were used. A second order PDE was implemented to simulate the Laplacian equation with the WM and CSF voxels adjacent to the boundaries of the gray matter set to fixed potentials. The Laplace equation was then solved in the gray matter volume. The solution $f(x, y, z)$ was a scalar field which divided the cortex into a set of equipotential sublayers.

The gradient of the Laplace solution was then computed and normalized to obtain a vector field perpendicular to the equipotential streamlines generated by the Laplace equation. The length of the trajectories going through each voxel was computed using a pair of first order linear partial differential equations as proposed by Yezzi and Prince.[12]

Let $L_0(x, y, z)$ be a function that measures the arc length of the trajectory from the inner boundary to an arbitrary point $\mathbf{p}$ with coordinates *(x,y,z)* in the gray matter, $L_1(x, y, z)$ the arc length of the trajectory from

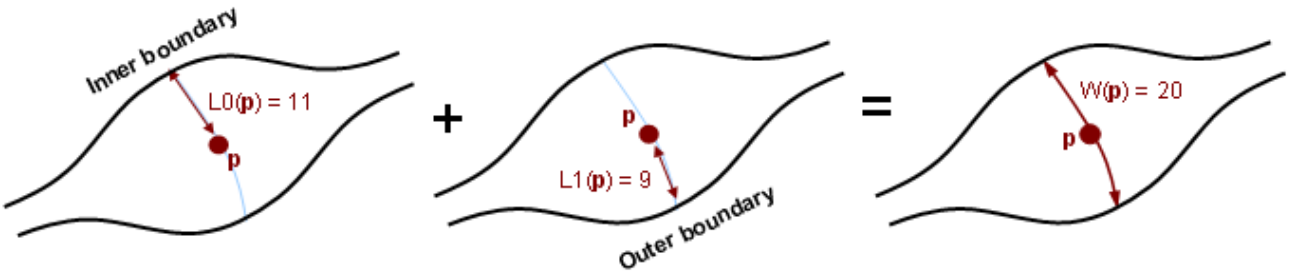

Figure 2. The distance equation.

the outer boundary to $\mathbf{p}$, and $\vec{T}$ the unit vector that is tangent to the streamline passing through $\mathbf{p}$. The total length W of the trajectory passing through the point $\mathbf{p}$ could be estimated as the sum of L_0 and L_1 (Figure 2), and defined the thickness of the cortex at every point $\mathbf{p}$:

$$W(x, y, z) = L_0(x, y, z) + L_1(x, y, z) \tag{5}$$

Since the distance between adjacent voxels was measured from the center of the voxel, a correction factor was included that took into account anisotropic resolution:

$$L_0(inner) = L_1(outer) = -\left(\frac{a+b+c}{6}\right) \tag{6}$$

where the spacing between neighboring voxels in the x, y and z directions were a, b and c, respectively. This shifted the measurement from the edge to the center of the voxel.

2.4 Improvement of the thickness estimation using fractional content

Initialization of boundaries to half of the negative mean voxel spacing (Equation 6) considered that there is no partial volume effect and that the boundaries between different tissues were infinitely sharp. As stated by previous works[1,2] this assumption limits greatly accuracy, especially when measuring GM thickness where two voxels are subject to PVE out of the 3 or 4 along the thickness of the cortex. A more accurate initialization of the boundaries L_0 and L_1 should take into account partial volume. Moreover, the fractional content of the different tissues should be measured along the boundaries.

This constraint can be added to the thickness estimation framework in a simple manner, by using the fractional content computed in 4. For every boundary voxel, the fractional content from (Equation 4) was added to half of the negative mean voxel spacing in order to shift the point where the thickness measure started according to the presence or absence of partial volume effect. For a voxel i along the GM/CSF boundary the initialization became

$$L_{1_i} = -\left(\frac{a+b+c}{6}\right) + f_{GM_i} \tag{7}$$

and along the GM/WM boundary became

$$L_{0_i} = -\left(\frac{a+b+c}{6}\right) + f_{GM_i} \tag{8}$$

where f_{GM} was given by 4.

For a resolution of 1 mm, if the PVE is not taking into account the initialization of the cortical thickness with the original method would be set to -0.5 at the boundary voxels. The next voxel in the direction of the

	Noise 0%	Noise 1%	Noise 3%	Noise 5%	Noise 7%	Noise 9%
GM	0.2	0.17	0.08	0.07	0.08	0.1
WM	0.04	0.02	0.01	0.02	0.05	0.09
CSF	0.24	0.27	0.28	0.31	0.33	0.35

Table 1. Average RMS error per level of noise of the fractional content of PV voxels.

cortex would then be computed to be +0.5 after integrating the trajectory (assuming $\vec{T}$ is parallel to one axis). This would result in a virtual boundary exactly at the border between the two voxels. With our extension, if the boundary voxel is found to contain 10% of gray matter, we would initialize it to -0.5-0.1=-0.6, effectively shifting the boundary to account for the PVE.

3. EXPERIMENTS AND RESULTS

Experiments were focused in validating three important points: 1) accuracy of the fractional content computation and PV labeling, 2) accuracy of the thickness measurement using PV estimation, and 3) reproducibility of our new measurement technique.

3.1 Fractional content and PV Validation

Experiments were performed on Brain Web simulated data set[16] to evaluate the accuracy of the fractional content computation and PV labeling. The images had an isotropic voxel resolution of $1mm^3$ and varying degrees of noise and intensity inhomogeneity. Evaluation was performed by comparing the resulting PV maps to the ground truth fractional volumes[16] using the RMS error.

In order to decrease computing time, we limited the computation of the PV to a region formed by a dilated gray matter (radius 4). Low average values of the computed RMS error (Table 1) demonstrated that most of the partial volume effect occurred along tissue boundaries, validating our area limitation for PV labeling. A higher RMS error for CSF was attributed to the fact that the mixture between CSF and background was not considered. Since this boundary was not taken into account in our thickness measurement the large error that we found were without consequences.

3.2 Accuracy of the thickness measurement

Experiments with synthetic spherical shells were performed to determine accuracy of the thickness measurement using PV estimation. Perfect sphere could not be generated on a discrete grid. For our experiment, we generated hollow sphere on a very high resolution grid (10 times greater than the final grid size) that we downsampled to similar MRI brain resolution to simulate partial volume effect. In summary to generate hollow partial volumed sphere images with size $r_x \times r_y \times r_z$ we performed the following steps:

1. A hollow sphere with inner radius r and external radius R was constructed on a grid size 1100x1100x1100 with resolution $(r_x/10) \times (r_y/10) \times (r_z/10)$. Voxels inside the hollow sphere were labelled 1, whereas those outside were set to 0. This simulated a hollow sphere with a thickness similar to the one of the brain cortex, $R - r = 3mm$.
2. The image was downsampled by averaging voxels to obtain a new volume with resolution $r_x \times r_y \times r_z$.
3. Partial volume for every voxels of the low resolution phantom could be estimated directly from its intensity with values between 0 and 1.

The comparison of the thickness estimation method with and without using PV estimation over spherical shells is shown on Table 2. The error caused by the partial volume effects on the sphere mean thickness were significantly reduced with our new method. For a 1 mm^3 resolution image the error was reduced from 6.66% to 2.33%. The results also show that the PV estimation produced accurate results for both isotropic and anisotropic data and that the accuracy was proportional to the image resolution.

Resolution	No PV Estimation Mean ± SD	PV Estimation Mean ± SD
0.5x0.5x0.5	2.86 ± 0.08	3.02 ± 0.05
0.5x0.5x1	2.80 ± 0.16	3.02 ± 0.15
1x1x1	2.72 ± 0.17	3.07 ± 0.10
1x1x1.5	2.68 ± 0.24	3.07 ± 0.20

Table 2. Accuracy comparison. Synthetic spherical shells 3 mm thick were generated to compare accuracy of the thickness estimation with and without using PV estimation.

	Mean ± SD (No PV Estimation)	Mean ± SD (PV Estimation)
Image 1	3.23 ± 1.61	3.33 ± 1.41
Image 2	3.18 ± 1.54	3.33 ± 1.36
Image 3	3.18 ± 1.54	3.31 ± 1.35
Overall	3.20 ± 0.03	3.32 ± 0.01

Table 3. Comparison of mean cortical thickness on three scans of the same subject with and without using PV estimation.

3.3 Reproducibility of the thickness measurement

Actual patient MRI were used for testing the reproducibility of our technique. The mean cortical thickness was computed across T1-weighted images of a subject scanned three times the same day. The results (Table 3) show that our approach is very reproducible with a smaller standard deviation compared to the original method without PV estimation. In addition the obtained mean values with PV estimation were considerably higher than with the original method. This behavior was consistent with our validation experiments on hollow spheres, and was expected since our approach compensated mis-detection of gray matter over the tissue boundaries by shifting the initialization values of L_0 and L_1. Figure 3 shows results obtained at different stages of the process.

4. DISCUSSION AND CONCLUSIONS

We presented an improvement of voxel-based cortical thickness estimation that used PV estimation in order to improve accuracy and reproducibility. The definition of thickness was based on the solution of the Laplace equation[11] simulated in the GM. In the original method it was assumed that tissue interfaces were sharp neglecting partial volume effect. Previous studies[1,2] have shown that excluding these effects over the boundaries could lead to a significant degradation of measurement accuracy in volume measurement. Our new approach uses a probabilistic modeling of partial voluming along boundaries in order to improve the accuracy of the cortical thickness measurement.

We performed validation of the PV estimation on synthetic phantom. Results on spherical hollow sphere showed that the error in thickness measurement was considerably reduced when the partial volume was taken into account. In addition, results on actual patients brain MRI allowed us to validate the reproducibility of the method. In the near future we plan to validate our method over a large database of patients from the Alzheimer's Disease Neuroimaging Initiative (ADNI) study.[18]

Boundary voxels initialization correction was performed assuming that the tissue interface was parallel to one of the edges of the voxel. This could generate small inaccuracies for complicated folding of the brain cortex especially for anisotropic data. Future work will combine the PV estimation with the direction of the tangent vector fields to determine accurately the tissue interface position for the initialization of the distance equation. Mis-segmented sulci results in an overestimation of cortical thickness. Use of PV estimation over regions with abnormal thickness can provide a way to detect sulci and reduce this effect on the overall accuracy of the technique.

In conclusion, we present an original approach to embed PV computation inside cortical thickness estimation. Results showed an increase in accuracy and precision of the thickness measurements. Our experiments over synthetic hollow spheres showed a diminution of the error of 4.33% and experiments over patient data show an improvement on the reproducibility of the measurement.

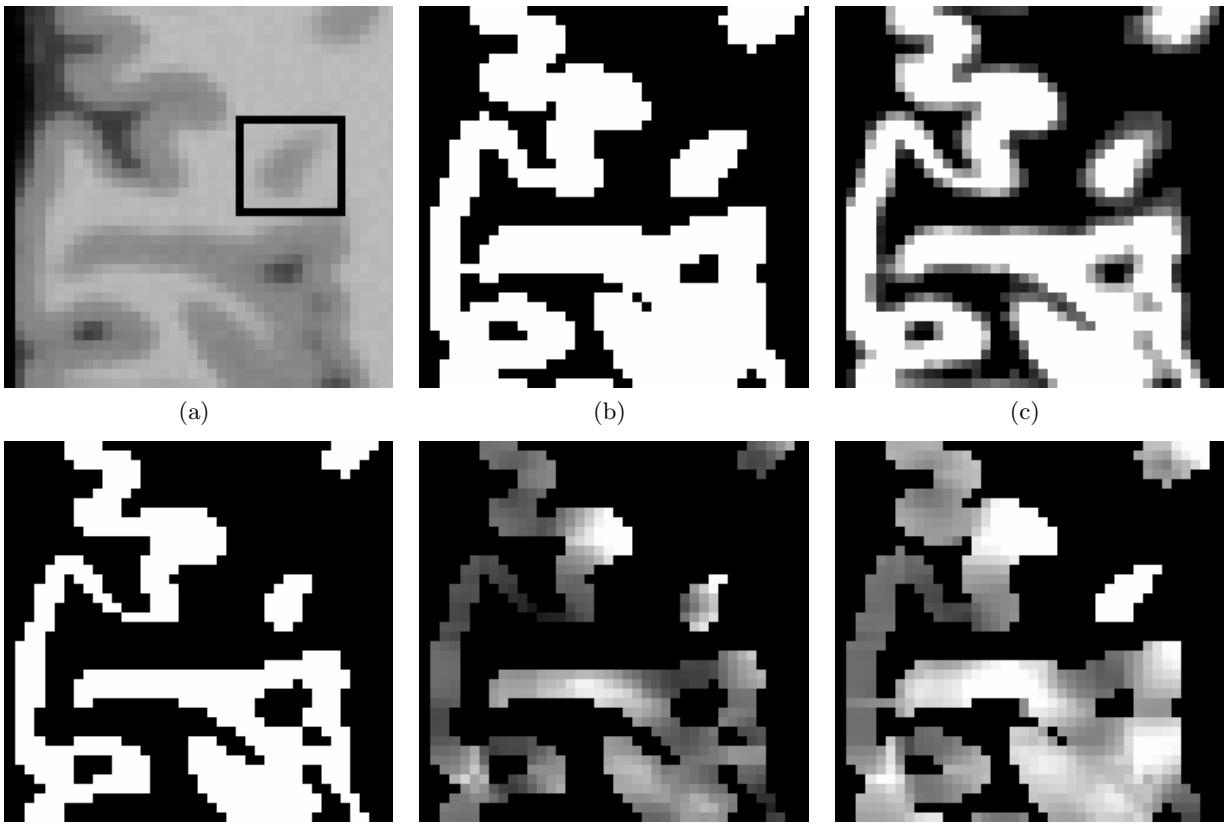

Figure 3. Example of PV estimation use on the cortical thickness measurement. Marked area over a slice of the original image (a) contains a high level of PV effect. Initial GM hard segmentation (b) classifies PV voxels as GM. PV Map of GM (c) detects the PV voxels allowing the refinement of the original segmentation (d). According to experimental measures of the cortex,[17] resulting thickness map (e) (black is 0 mm thickness, white is 7 mm) obtains a more accurate measure than the thickness map without PV estimation (f).

REFERENCES

1. W. Niessen, K. Vincken, J. Weickert, B. T. H. Romeny, and M. Viergever, "Multiscale segmentation of three-dimensional MR brain images," *International Journal of Computer Vision* **31**(2), pp. 185–202, 1999.
2. M. González-Ballester, A. Zisserman, and M. Brady, "Segmentation and measurement of brain structures in MRI including confidence bounds," *Medical Image Analysis* **4**(3), pp. 189–200, 2000.
3. H. Choi, D. Haynor, and Y. Kim, "Partial volume tissue classification of multichannel magnetic resonance images - a mixel model," *IEEE Trans. Med. Imag.* **10**(3), pp. 395–407, 1991.
4. L. Nocera and J. Gee, "Robust partial volume tissue classification of cerebral MRI scans," in *SPIE Medical Imaging*, K. Hanson, ed., **3034**, pp. 312–322.
5. D. Pham and J. Prince, "Unsupervised partial volume estimation in single-channel image data," in *Proc. IEEE Workshop Mathematical Methods in Biomedical Image Analysis-MMBIA'00*, pp. 170–177, 2000.
6. P. Santago and H. Gage, "Quantification of MR brain images by mixture density and partial volume modeling," *IEEE Trans. Med. Imag.* **12**(3), pp. 566–574.
7. D. Laidlaw, K. Fleischer, and K. Barr, "Partial-volume Bayesian classification of material mixtures in MR volume data using voxel histograms," *IEEE Trans. Med. Imag.* **17**(1), pp. 74–86, 1998.
8. D. Shattuck, S. Sandor-Leahy, K. Schaper, D. Rottenberg, and R. Leahy, "Magnetic resonance image tissue classification using a partial volume model," *Neuroimage* **13**(5), pp. 856–876, 2001.
9. A. Noe and J. C. Gee, "Efficient partial volume tissue classification in mri scans," in *Medical Image Computing and Computer-Assisted Intervention - MICCAI 2002: 5th International Conference Proceedings, Part I*, *LNCS* **2488/2002**, pp. 698–705, 2002.
10. J. Tohka, A. Zijdenbos, and A. Evans, "Fast and robust parameter estimation for statistical partial volume models in brain MRI," *NeuroImage* **23**, pp. 84–97, 2004.
11. S. Jones, B. Buckbinder, and I. Aharon, "Three-dimensional mapping of cortical thickness using Laplace's equation," *Human Brain Mapping* **11**(1), pp. 12–32, 2000.
12. A. Yezzi and J. Prince, "An Eurelian PDE approach for computing tissue thickness," *IEEE Trans. Med. Imag.* **22**, pp. 1332–1339, 2003.
13. V. Singh, H. Chertkow, J. P. Lerch, A. C. Evans, A. E. Dorr, and N. J. Kabani, "Spatial patterns of cortical thinning in mild cognitive impairment and alzheimer's disease," *Brain* **129**, pp. 2885–2893, 2006.
14. K. V. Leemput, F. Maes, D. Vandermeulan, and P. Suetens, "Automated model-based tissue classification of MR images of the brain," *IEEE Trans. Med. Imag.* **18**(10), pp. 897–908, 1999.
15. J. Besag, "On the statistical analysis of dirty pictures," *Journal of the Royal Statistical Society, Series B* **48**(3), pp. 259–302, 1986.
16. R.-S. Kwan, A. Evans, and G. Pike, "An extensible MRI simulator for post-processing evaluation," in *Visualization in Biomedical Computing (VBC'96)*, *LNCS* **1131**, pp. 135–140, 1996.
17. X. Zeng, L. Staib, R. Schultz, and J. Duncan, "Segmentation and measurement of the cortex from 3d MR images using coupled-surfaces propagation," *IEEE Trans. Med. Imag.* **18**(10), pp. 927–937.
18. http://www.nia.nih.gov/Alzheimers/ResearchInformation/ClinicalTrials/ADNI.htm.